Respiratory adaptations in a deep-sea orbiniid polychaete from Gulf of Mexico brine pool NR-1: metabolic rates and hemoglobin structure/function relationships

Stéphane Hourdez[1,2,*], Roy E. Weber[3], Brian N. Green[4], John M. Kenney[5] and Charles R. Fisher[1]

[1]Department of Biology, 208 Mueller Lab, Pennsylvania State University, University Park, PA 16802, USA, [2]Station Biologique de Roscoff, BP74, CNRS-UPMC-INSU, 29682 Roscoff cedex, France, [3]Center for Respiratory Adaptation (CRA), Department of Zoophysiology, University of Aarhus, 8000 Aarhus C, Denmark, [4]Micromass Ltd, Tudor Road, Altrincham, Cheshire WA14 5RZ, UK and [5]Institute for Storage Ring Facilities – Aarhus (ISA), University of Aarhus, 8000 Aarhus C, Denmark

*Present address: Department of Biology, 208 Mueller Lab, Pennsylvania State University, University Park, PA 16802, USA
(e-mail: hourdez@psu.edu)

Summary

Methanoaricia dendrobranchiata Blake (Polychaeta; Orbiniidae) occurs in large numbers in association with communities of the mussel Bathymodiolus childressi at hydrocarbon seeps on the Louisiana Slope of the Gulf of Mexico. Its microhabitat can be strongly hypoxic (oxygen is often undetectable) and sulfidic (sulfide concentrations can reach millimolar levels), which may seriously challenge aerobic metabolism. We describe a suite of adaptations to its low-oxygen environment. The worms are capable of regulating their rate of oxygen consumption down to partial pressures of approximately 870 Pa oxygen. This capability correlates with a large gill surface area, a small diffusion distance from sea water to blood, a very high hemoglobin oxygen-affinity (P_{50}=27.8 Pa at 10 °C and pH 7.6) and a Bohr effect that is pronounced at high oxygen saturations. When fully saturated, the hemoglobin binds sufficient oxygen for only 31 min of aerobic metabolism. However, these polychaetes can withstand extended periods of anoxia both in the absence and presence of $1\,mmol\,l^{-1}$ sulfide (TL_{50}=approx. 5.5 and 4 days, respectively).

Key words: hypoxia, anoxia-tolerance, sulphide-tolerance, functional properties, cold seep, oxygen consumption, physiology, haemoglobin, orbiniid, polychaete, *Methanoaricia dendrobranchiata.*

Introduction

Metazoan communities thriving on local chemolithoautotrophic and methanotrophic primary production were discovered in 1984 by the Geochemical and Environmental Research Group (GERG) on the Louisiana Slope of the Gulf of Mexico (Kennicutt et al., 1985; Brooks et al., 1987). Extensive beds of the methanotrophic symbiont-containing mussel *Bathymodiolus childressi* occur at many sites in the area (Childress et al., 1986; MacDonald et al., 1990a,b; Nix et al., 1995). *Methanoaricia dendrobranchiata* Blake (Polychaeta; Orbiniidae) occurs with the mussels at most of the sites and is particularily abundant in the mussel bed around Brine Pool NR1 (Macdonald et al., 1990c), where it occurs either individually or in tight aggregations of as many as 150 worms (Smith et al., 2000; Hourdez et al., 2001). The worms often extend the anterior part of their body above the mussels into the overlying water (Fisher, 1996; Hourdez et al., 2001).

At Brine Pool NR1, the mussel bed rings the edge of the hypersaline pool on unconsolidated sediments saturated with brine. The oxygen concentration in water sampled between the mussels averaged $39\,\mu mol\,l^{-1}$ and was often undetectable by gas chromatography ($<5\,\mu mol\,l^{-1}$; Smith et al., 2000). Although no sulfide could be detected in the brine pool itself, millimolar levels are present in the brine-saturated sediments under the outer edge of the mussel bed (Smith et al., 2000). The combination of sulfidic and hypoxic conditions presents a major respiratory challenge for active metazoans (Somero et al., 1989; Grieshaber and Völkel, 1998). Similar conditions characterize the microhabitats of many hydrothermal vent communities (Johnson et al., 1988; Fisher et al., 1988a,b; Sarrazin and Juniper, 1999).

Several studies on hydrothermal vent polychaetes have shown larger mass-specific gill surface areas and shorter diffusion distances between the environment and the body fluids than in related genera from other environments (Jouin and Gaill, 1990; Hourdez and Jouin-Toulmond, 1998). The gills of *M. dendrobranchiata* are also hypertrophied compared with those of other orbiniids and resemble those of the vent

polychaetes (Hourdez et al., 2001). This characteristic and the short diffusion distance across the gill epithelia have been interpreted as adaptations for life in a hypoxic environment (Jouin and Gaill, 1990; Jouin-Toulmond et al., 1996; Hourdez and Jouin-Toulmond, 1998; Hourdez et al., 2001).

In addition to these anatomical adaptations, the respiratory pigments of the vent polychaetes and vestimentiferan species studied to date have very high oxygen affinities and strong Bohr effects that may facilitate oxygen uploading in the gills at low oxygen tensions as well as its release in the tissues (Arp et al., 1990; Toulmond et al., 1990; Hourdez et al., 1999). *M. dendrobranchiata* contains an extracellular hemoglobin in its blood vessels (Hourdez et al., 2001). In annelids, such extracellular hemoglobins are usually giant hexagonal bilayer (HBL) molecules, made up of 12 large subunits (dodecamers) composed of globin chains. These dodecamers are held together by polypeptide chains known as linkers (for a review, see Lamy et al., 1996).

We studied aspects of the respiratory physiology of *M. dendrobranchiata* from the cold seeps of the Gulf of Mexico. The relationship between oxygen consumption rate and environmental oxygen concentration was determined together with tolerance of anoxia in both the presence and absence of sulfide. We also determined the concentration of hemoglobin in the worms and describe the molecular and functional properties of the purified molecule. Finally, these findings are discussed in the context of the animal's habitat and behavior.

Materials and methods
Animal collection

Specimens of *Methanoaricia dendrobranchiata* Blake were collected together with mussels at the Brine Pool NR-1 site on the Louisiana Slope in the Gulf of Mexico (23°43′24″N, 91°16′30″W at 650 m depth; MacDonald et al., 1990c; Smith et al., 2000) in July 1998 using the scoop collector on the arm of the submersible *Johnson Sea-Link I*. The animals were placed in a temperature-insulated box on the submarine for recovery by the *RV Edwin Link*, where they were transferred to aquaria of chilled (8 °C) aerated sea water for between 1 and 7 days before use in oxygen consumption and anoxia experiments. There were no apparent adverse effects of maintenance at ambient pressure or normoxia on *M. dendrobranchiata*, which have been maintained alive in the laboratory, with mussels, for over a year.
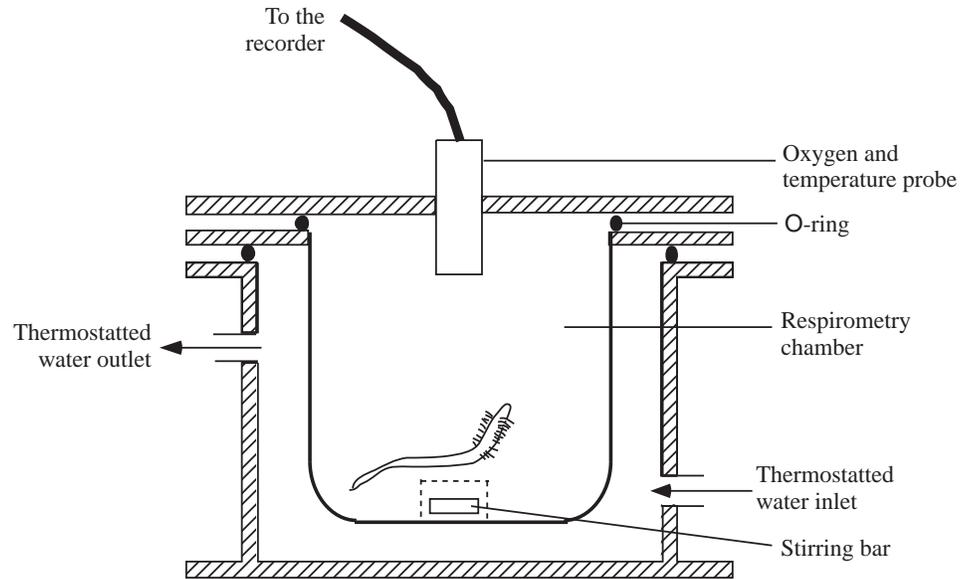

Fig. 1. Experimental apparatus used for respiration measurements at controlled temperature.

Oxygen consumption rates

The oxygen consumption rates of individual worms were determined in water-jacketed, gas-tight chambers (Fisher et al., 1985) at 8.5±0.5 °C using Clark-type oxygen probes (Orion 835 dissolved oxygen meter) (Fig. 1). Oxygen concentrations in the chamber were recorded every 5 min for 16–17 h. After the experiment, the worms were rapidly dried with paper tissues and frozen in cryovials for transport to Pennsylvania State University. To determine the wet mass of the worm, the cryovial was weighed before and after removing the worm. Mass-specific oxygen consumption rates were calculated for each 20-min interval (using five data points) and plotted against the mean oxygen concentrations for that time interval.

Anoxia and sulfide-tolerance

Worms were maintained anaerobically in water containing 0, 0.06 or 1 mmol l^{-1} sulfide to determine their tolerance to anoxia under these conditions. Oxygen-free sea water was obtained by bubbling with nitrogen for 30 min and then transferred to a nitrogen atmosphere in a glove bag in a cold room at 8 °C, where all subsequent manipulations were conducted. The absence of detectable oxygen was confirmed with a dissolved oxygen meter (Orion 835). Pre-weighed washed crystals of sodium sulfide were then added, and the sulfide concentrations were measured by gas chromatography (Childress et al., 1984). Individual worms were incubated separately in sealed 30 ml glass scintillation vials secondarily contained in a 500 ml gas-tight container filled with nitrogen-equilibrated water (to dampen minor temperature fluctuations and maintain anaerobic conditions). Eleven vials containing one worm each were incubated anaerobically under each experimental condition, and an additional 22 worms from the same collection were kept

under normoxia in individual vials that were open to the atmosphere (controls). Survival was checked every 12 h until the ship reached port (7 days).

To evaluate the time corresponding to a 50 % survival rate (TL_{50}), the following survival curve was fitted to the data:

$$s = \frac{100}{1 + (t/TL_{50})^b} \, , \tag{1}$$

where s is the percentage of survivors, t is time and b is a sigmoidicity coefficient. Iterations were repeated using the program DeltaGraph 4.5 until the parameters TL_{50} and b did not vary by more than 1 %.

Extraction and purification of hemoglobin

Because of the very small blood vessels, it was not possible to sample pure blood intravascularly. Approximately 75 worms from a single collection were batch-frozen 1 h after recovery for shipment to the laboratory and hemoglobin extraction. In the laboratory, the worms were homogenized with 100 ml of extraction buffer (50 mmol l^{-1} Tris, pH 8, 1 mmol l^{-1} EDTA and 1 μmol l^{-1} phenylmethanesulfonic fluoride, PMSF). The homogenate was centrifuged for 20 min at 20 000 g to remove the coarse debris. The bright red supernatant was then centrifuged at 100 000 g for 5 h to pellet the hemoglobin. The pellet containing the hemoglobin was resuspended in 1 ml of the extraction buffer, and the hemoglobin was purified by fast protein liquid chromatography (FPLC) on a Superose 6 column (10 mm×300 mm; Pharmacia Inc., 5–5000 kDa separation range) using 400 mmol l^{-1} NaCl, 2.95 mmol l^{-1} KCl, 32 mmol l^{-1} MgSO$_4$, 11 mmol l^{-1} CaCl$_2$ and 50 mmol l^{-1} Hepes at pH 7.0 as the elution buffer. The elution rate was typically 0.5 ml min^{-1}, and the elutant was monitored at 280 nm. The molecular mass of the collected fractions was estimated using a sample of *Riftia pachyptila* blood, which contains four peaks of known molecular mass (Zal et al., 1996). The presence of hemoglobin in colored fractions was verified on the basis of peak absorptions near 414 nm.

Hemoglobin content

To assess the significance of the hemoglobin for oxygen storage, 61 worms ranging widely in size (0.08–1.95 g) were individually frozen on board ship. In the laboratory, they were weighed and homogenized individually, using a ground-glass tissue homogenizer, in 1 mmol l^{-1} Tris buffer, pH 8, containing 1 mmol l^{-1} EDTA and 1 μmol l^{-1} PMSF to prevent hydrolysis by proteases. The homogenate was centrifuged at 10 000 g for 15 min to remove cellular debris, and the supernatant was used for heme concentration measurements after appropriate dilution of the samples in the extraction buffer. Potassium ferricyanide solution (10 mmol l^{-1}; 10 ml) was added to 2 ml of this diluted solution, which had been incubated for 5 min at room temperature to oxidize the hemoglobin completely to methemoglobin. Potassium cyanide (50 mmol l^{-1}; 10 ml) was then added to obtain the cyan-methemoglobin derivative, which was quantified on the basis of the absorbance of the

solution at 540 nm and the most appropriate published extinction coefficient of 11.01 mmol^{-1} cm^{-1} (Van Assendelft, 1970).

Negative-stain transmission electron microscopy of purified, whole hemoglobin molecules

Images of negatively stained *M. dendrobranchiata* hemoglobin molecules were recorded by transmission electron microscopy to assess their molecular organization following a method modified from Valentine et al. (1968). Diluted purified hemoglobin (3 μl; 0.037 mmol l^{-1} heme in 100 mmol l^{-1} Tris buffer at pH 6.85) was applied to a very thin (10–30 nm) carbon foil supported on a standard 3.05 mm copper electron microscopy grid. After allowing 1 min for the hemoglobin molecules to adhere to the carbon foil, 6 μl of 2 % (m/v) uranyl acetate solution was applied to stain the molecules. After 10 s, the grid with the stained sample was blotted with Whatman filter paper, leaving only a very thin wet layer on the carbon foil, which was allowed to dry in air. The negatively stained specimens were examined using a Philips CM120 electron microscope at 100 keV, and images were recorded under minimum-dose conditions (Kenney et al., 1995) at 40 000× magnification.

The transmission electron microscopy images of the negatively stained hemoglobin molecules were analyzed to reveal the symmetry of their macromolecular structure. The images were digitized, and individual hemoglobin molecules were selected and centered by reference free alignment using the program SPIDER (Frank et al., 1996). The rotational frequency analysis of SPIDER-processed images was performed using the Medical Research Council image-processing programs (Crowther et al., 1996), and the rotational power spectra of the images were calculated.

Electro-spray ionization mass spectrometry

Electro-spray ionization mass spectrometry (ESI-MS) was used under denaturing conditions to determine the molecular masses of the chains and covalently bound subunits present in the native hemoglobin and in the 210 kDa fraction (see Results). Three different treatments were applied to this hemoglobin sample to analyze its structure, as described previously (Green et al., 1996, 1999): (i) carboxyamidomethylation (Cam) to determine the number of free cysteines, (ii) reduction with dithiothreitol (DTT) to determine the composition of dimeric species and the reduced masses of the chains, and (iii) reduction plus Cam (reduced/Cam), to determine the total number of cysteine residues in each chain. The DTT reduction was carried out at a concentration of 5 mmol l^{-1} for 2 min at 20 °C. Briefly, samples were introduced at a rate of 5 μl min^{-1} into the electrospray source of a Quattro LC mass spectrometer (Micromass UK Ltd). They were analyzed at a concentration of 0.25–0.5 mg ml^{-1} in 1:1 (by volume) acetonitrile:water containing 0.2 % formic acid. The scan range was m/z 600–2500, and the cone voltage (counter electrode to skimmer voltage) ramp was from 30 V at m/z 600 to 100 V at m/z 2500

(m is mass; z is charge). Mass scale calibration employed the multiply charged series of ions from horse heart myoglobin (M_r 16 951.5 Da; Sigma, M-1882). Data were processed using the Maximum Entropy (MaxEnt)-based software supplied with the instruments. Molecular masses are based on the atomic masses of the elements: C=12.011, H=1.00794, N=14.00674, O=15.9994 and S=32.066 (IUPAC).

Oxygen equilibrium curves

Equilibrium curves were obtained with a diffusion chamber apparatus (Sick and Gersonde, 1969) modified as described previously (Weber, 1981). Briefly, small (4 μl) samples of purified hemoglobin were equilibrated with pure (>99.998 %) N_2 and O_2 and mixtures of these gases and air prepared using Wösthoff pumps. The pH of the hemoglobin solutions was varied by adding 6 μl of 1 mol l^{-1} Bis-Tris Propane buffer of a range of pH values to 100 μl aliquots of the sample, and water was added to bring the total volume to 120 μl. The pH was measured in duplicate with a blood gas analyzer (BMS2, Radiometer) on 50 μl subsamples. Oxygen equilibrium and pH measurements were carried out at 10, 20 and 30 °C (±0.1 °C).

Values of P_{50} (the P_{O_2} at which the hemoglobin is half-saturated with oxygen) and n_{50} (cooperativity at P_{50}) were derived from linear regression Hill plots of $\log[Y/(1-Y)]=f(\log P_{O_2})$ for S (saturation values) of 30–70 %. The Bohr factor (Φ) was calculated as $\Phi=\Delta\log P_{50}/\Delta pH$, and the apparent heat of oxygenation was calculated as $\Delta H^{obs}=2.303R\Delta\log P_{50}/[(1/T_1)-(1/T_2)]$, where R is the gas constant and T_1 and T_2 are the absolute temperatures. The value thus obtained (ΔH^{obs}) comprises the intrinsic heat of oxygenation (ΔH^{intr}), the heat of solution of O_2 (ΔH^{sol}, approximately 13 kJ mol^{-1}) and contributions from oxygenation-linked processes such as the heats of reaction with protons and other effectors. In the absence of oxygenation-linked binding of protons (when $\Phi=0$) and other allosteric effectors, $\Delta H^{intr}=\Delta H^{obs}-\Delta H^{sol}$ (see Wyman et al., 1977).

Values reported as means ± standard deviation (S.D.) throughout this manuscript.

Results
Rates of oxygen consumption

Fig. 2A shows the reduction in oxygen concentration from 4 to 0.1 mg l^{-1} (partial pressure decreasing from 10 000 to 260 Pa) recorded in the incubation chamber for a worm 1.24 g in wet mass. The calculated oxygen consumption rates for this experiment are shown in Fig. 2B. The oxygen consumption rate is relatively constant (0.66±0.08 μl O_2 min^{-1} g^{-1} wet mass, N=75 points) for oxygen levels between normoxia and 0.5 mg l^{-1} (P_{O_2}=1300 Pa). Below the critical value of 0.5 mg l^{-1} (P_{O_2}=1300 Pa), oxygen consumption rate decreases gradually and ceases at a concentration of 0.1 mg l^{-1} (P_{O_2}=260 Pa). The small variations in the mean oxygen consumption rate at the beginning of the incubation are interpreted as periods of activity and rest.

A logistic curve was found to describe the data best on the basis of the χ^2-value:

$$\dot{V}_{O_2}=\frac{a([O_2]-c)}{\{1+b([O_2]-c)\}},\qquad(2)$$

where $[O_2]$ is in mg l^{-1} and c is the value of $[O_2]$ at which the oxygen uptake rate ($\dot{V}_{O_2}$) is zero, and a and b are constants. When P_{O_2} tends to infinity, $\dot{V}_{O_2}$ tends to a/b, which is the maximum oxygen consumption rate ($\dot{V}_{O_2max}$). The constants a and b describe the initial slope and, thereby, how fast the plateau is reached. For the worm depicted in Fig. 2B, a=6.146, b=8.705 ml μl^{-1} O_2 and c=0.106 μl O_2 ml^{-1}. The maximum oxygen consumption rate, $\dot{V}_{O_2max}$, is then 0.706 μl O_2 min^{-1} g^{-1} wet mass.

Separate linear regressions for points below 0.4 mg O_2 l^{-1} and points above 1.5 mg O_2 l^{-1} allowed us to estimate the critical pressure (the intercept of the two lines). For the worm in Fig. 2, the intercept gives a critical pressure P_c of 0.27 mg O_2 l^{-1} (700 Pa).

These measurements were made for seven worms ranging from 0.64 to 1.87 g in wet mass. For two of these experiments, the oxygen concentration did not fall below 1 mg l^{-1}. In these cases, we used the linear portion of the oxygen concentration as a function of time curve (Fig. 2A) to calculate the oxygen consumption rate. For the five other experiments, the shape of the curve was always the same, and the χ^2-value supported the use of the above equation for each data set (P<0.01). The P_c values ranged from 0.25 to 0.38 mg O_2 l^{-1} in the five experiments (P_{O_2}=650–990 Pa) and oxygen consumption ceased at 0.09–0.11 mg O_2 l^{-1} (P_{O_2}=230–280 Pa).

Fig. 3 shows the relationship between respiratory rate and animal wet mass. The oxygen consumption rate follows a power function trend described by the equation:

$$\dot{V}_{O_2}=0.488M^{-0.702},\qquad(3)$$

where $\dot{V}_{O_2}$ is the oxygen consumption rate (in μl O_2 min^{-1} g^{-1}) and M is the wet mass of the worm (in g). This curve fits the data with a correlation coefficient r^2 of 0.457 (P<0.1). This lack of significance is not surprising because the wet mass does not span an order of magnitude. The mean oxygen consumption rate for all the experiments is 0.479±0.160 μl O_2 min^{-1} g^{-1}.

Anoxia and sulfide-tolerance

Fig. 4 shows the percentage survival as a function of time under normoxia, anoxia, anoxia + 60 μmol l^{-1} sulfide and anoxia + 1 mmol l^{-1} sulfide. None of the normoxic (control) animals died during the experiment, while only a single worm survived for 7 days under anoxia. The mortality curves are sigmoidal. Curve-fitting yield TL_{50} values (time to reach 50 % survival) of 99.1, 119.6 and 133.5 h, respectively, for anoxia + 1 mmol l^{-1} sulfide, anoxia + 60 μmol l^{-1} sulfide and anoxia without sulfide. Analysis of covariance (ANCOVA) of the linearized data indicated that the effect of the treatment was highly significant, and pairwise comparisons confirmed that all TL_{50} values were significantly different (P<0.01).

Hemoglobin content

Fig. 5 shows the hemoglobin content as a function of wet mass for the 61 worms. The masses ranged from 0.008 to 1.95 g and the hemoglobin (Hb) contents from 143 to 373 nmol Hb g^{-1} wet mass. The individual mass-specific hemoglobin content (Q) increases with the size, reaching a plateau at approximately 250 nmol g^{-1} wet mass. The mean mass-specific hemoglobin content is 237±52 nmol Hb g^{-1} wet mass ($N=61$). The following equation fits the data, with a correlation coefficient $r=0.388$ ($N=61$, $P<0.01$):

$$Q = 0.256M^{0.056}. \quad (4)$$

Assuming complete saturation of hemoglobin and a constant oxygen consumption rate, the temporal significance of the oxygen store (A; in minutes) can be derived as $Q/\dot{V}_{O_2}$ (equations 4 and 3), which yields:

$$A = 0.524M^{0.758}. \quad (5)$$

For a 1 g worm, the fully saturated hemoglobin would then represent an oxygen store allowing 31 min of aerobic metabolism. A corresponding calculation using the mean oxygen consumption rate instead of equation 3 gives a very similar result (32 min).

Purification of the hemoglobin

The extracellular hemoglobin was purified by FPLC. Absorbances at 280 nm (which characterize proteins) and 414 nm (the Soret band, which characterizes hemoglobins) show two hemoglobin fractions with masses of approximately 3.5×10^6 Da and 210 kDa. The second fraction, which was very small (elution profile not shown), is referred to as 'dodecamers' (D in the figures) and is considered to be a dissociation product of the first fraction of whole hemoglobin molecules (W-Hb) (for an example, see Zal et al., 1996). Support for this designation is presented below.

Image analysis of transmission electron microscopy pictures of whole hemoglobin molecules

The transmission electron microscopy pictures of the whole hemoglobin molecules (Fig. 6A,B) showed a strong peak at the sixth rotational harmonic, indicating a sixfold rotation symmetry (Fig. 6C). This information was used to produce a rotationally Fourier-filtered image. The result is a typical top (sixfold axis) view of a hexagonal bilayer (HBL) (Fig. 6D).

Structure of the hemoglobin

Under denaturing conditions, ESI-MS of the native hemoglobin revealed three groups of peaks with molecular masses of approximately

16, 32 and 49 kDa. In the first group, four peaks can be distinguished: a1, a2, a3 and a4, with masses of 15 824.8, 15 835.1, 15 864.5 and 16 255.4±1.5 Da and relative intensities of 0.40:0.34:0.19:0.17, respectively ($N=5$) (Fig. 7A; Table 1). A single peak (Dm) occurred at 31 972.6±3.0 Da ($N=5$), while the third group consisted of four peaks (LD1–LD4) between 48 715.5 and 48 804.9 Da (Fig. 7, inset in A). Careful examination of the ESI spectra from several preparations of W-Hb analyzed under various conditions failed to reveal the presence of components that could correspond to trimers or tetramers of globin chains. ESI-MS on the 210 kDa fraction revealed peaks corresponding to a1–a4 and Dm only (no peaks of higher mass were seen).

Under mild reducing conditions (1 and 2 min in the presence of 5 mmol l^{-1} DTT at 22°C) (Fig. 7B), the masses of a1–a3 remained unchanged, while the mass of a4 decreased by 119.5 Da, suggesting that this chain is cysteinylated.
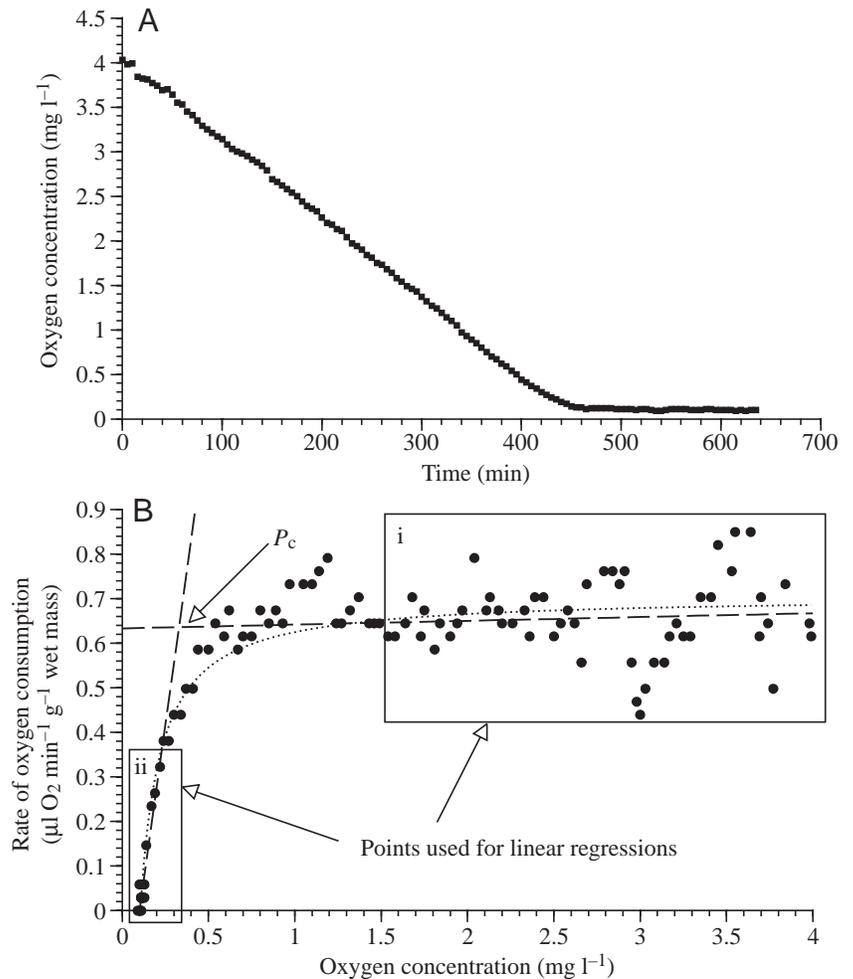

Fig. 2. Oxygen consumption for a specimen (1.24 g wet mass) of *Methanoaricia dendrobranchiata* at 8°C. (A) Changes in the oxygen concentration in the chamber during the experiment. Readings were taken every 5 min. (B) Calculated oxygen consumption rate as a function of oxygen concentration for the same worm. Regression (i): $r^2=0.006$, $N=54$, $P=0.589$; regression (ii): $r^2=0.903$, $N=20$, $P<0.0005$. P_c, critical pressure.
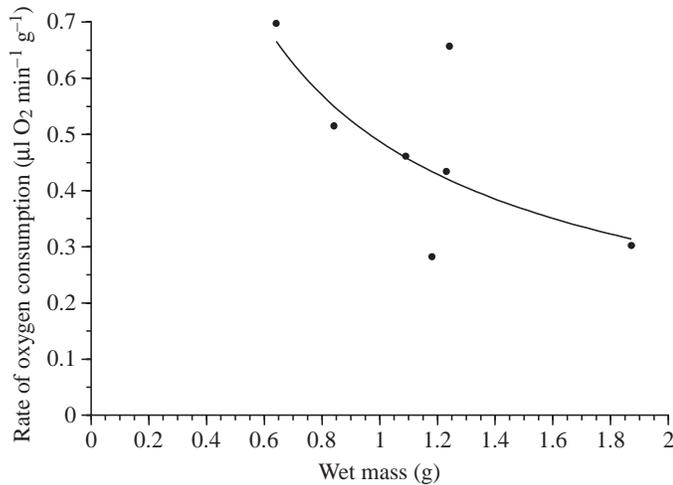
Fig. 3. Relationship between oxygen consumption rate and wet mass of *Methanoaricia dendrobranchiata*. The line fits the equation: $\dot{V}_{O_2}=0.488M^{-0.702}$, $r^2=0.457$, $P<0.1$.

Concomitantly, the intensity of the Dm peak decreased and the group of peaks around 49 kDa disappeared. In addition, several new peaks appeared: b, c and d at 15 373.4, 16 600.6 and 17 172.9 Da, respectively (±1.5 Da, $N=6$), and L1, L2, L3, L4 and L5 at 24 358.7, 24 379.0, 24 404.2, 26 279.3 and 27 687.1 Da, respectively (±3.0 Da, $N=4$). These results imply that Dm is a disulphide-bonded dimer composed of monomers b and c, since b+c−2H=31 972.0, which is the mass determined for Dm in the unreduced hemoglobin (Green et al., 1996). Furthermore, twice the masses of L1, L2 and L3 minus 2H are within experimental error of the masses of LD1, LD2 and LD4 (Fig. 7B), implying that L1–L3 exist as disulfide-linked dimers in the native hemoglobin. L1–L5 have masses that are typical of linker chains. However, no peaks were observed in the native hemoglobin that could correspond to dimers of L4 and
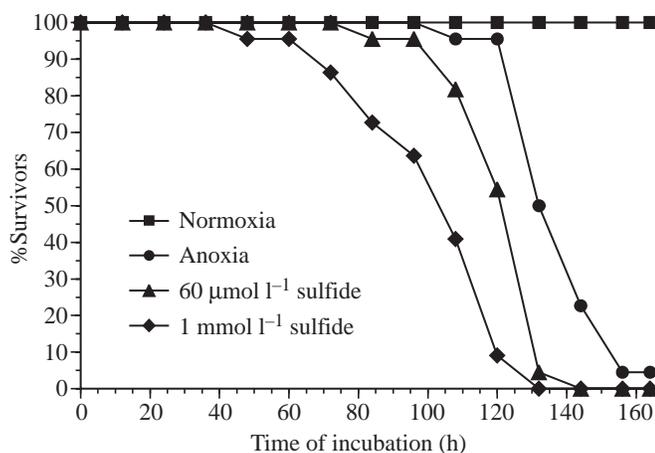

Fig. 4. Percentage survival of *Methanoaricia dendrobranchiata* under normoxia, anoxia, anoxia + 60 μmol l⁻¹ sulfide and anoxia +1 mmol l⁻¹ sulfide. Twenty-two worms were exposed to each condition.
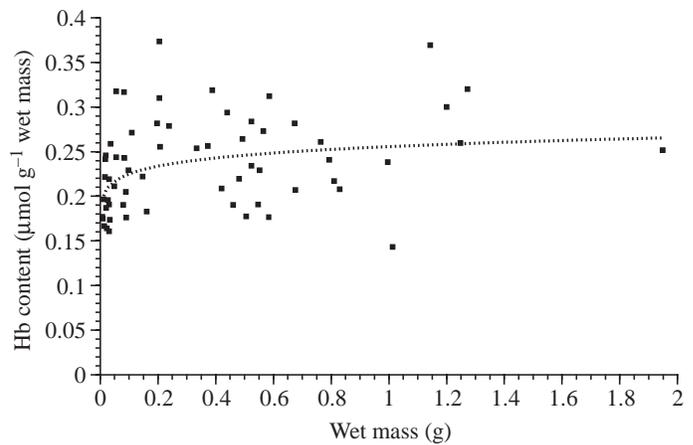

Fig. 5. Hemoglobin content as a function of wet mass for *Methanoaricia dendrobranchiata* ($N=61$). The dotted line fits the equation: $Q=0.256M^{0.056}$, $P<0.01$.

L5. Moreover, while L1–L3 remained present upon reduction, L4 and L5 disappeared, with the concomitant appearance of several relatively minor peaks in the range 18–23 kDa. Peak d cannot be assigned to a higher-mass component in the W-Hb. It is possible that it is one of the components in a dimer or higher-order multimer that was not detected in the denatured W-Hb. It could also correspond to a fragment of a linker, made more fragile after reduction.

After carboxyamidomethylation (Cam) with iodoacetamide, the masses of a1–a3 remained unchanged, indicating that they contain no free cysteine. However, the mass of Dm increased by 2 Cam units, implying that it contains two free cysteine residues. The total number of cysteine residues in each chain and the reduced masses of the chains were determined from the reduced/Cam hemoglobin, as shown in Table 1 and Fig. 7C. Strong support for LD1–LD4 being dimeric forms of L1–L3 is provided by the reduced/Cam results as follows. L1–L3 have masses typical of linker chains and appear to exist as dimers in the native hemoglobin. The peak at 48 715.5 Da is probably a dimer made of two L1 chains (2L1−22H=48 710.2 Da) and the peak at 48 755.1 Da could be a dimer made of two L2 chains, or one L1 chain and one L3 chain (2L2−22H=48 757.8 Da and L1+L3−22H=48 757.1 Da, respectively). The peak at 48 777.4 Da is probably a dimer of L2 and L3 (L2+L3−22H=48 780.9 Da) and, finally, the peak at 48 804.9 Da is probably a dimer of two L3 chains (2L3−22H=48 804.0 Da). All these calculated masses are well within the experimental error for the measured masses of the peaks.

Functional properties of the hemoglobin

In Fig. 8, the effects of pH on the affinity (P_{50}) and cooperativity (n_{50}) of the intact hemoglobin (W-Hb) and dodecamers (D) at 10, 20 and 30°C are shown. W-Hb and D exhibit the same oxygen affinities at pH 7.6 for 10°C ($P_{50}=27.8$ Pa), at pH 7.4 for 20°C ($P_{50}=82$ Pa) and at pH 7.1 for 30°C ($P_{50}=271$ Pa). At lower pH values, D shows

Table 1. *Molecular masses of the chains and subunits in orbiniid hemoglobin*

	Chain/subunit[a]	Mass (Da)[b]	Chain[b]	Mass (Da)[b]	Free Cys	Total Cys
Globins						
Monomer	a1	15 824.8	a1	15 827.8	0	2
Monomer	a2	15 835.1	a2	15 838.4	0	2
Monomer	a3	15 864.5	a3	15 866.8	0	2
Monomer	a4	16 255.4	a4-Cys	16 138.5	1	4
Dimer	Dm[c]	31 972.6			2	8
			b	15 375.7	–	4
			c	16 602.1	–	4
			d[d]	17 174.7	–	5
Linkers						
Dimers	LD1	48 715.5			0	22
Dimers	LD2	48 755.1				
Dimers	LD3	48 777.4				
Dimers	LD4	48 804.9				
			L1	24 366.2	–	11
			L2	24 390.0	–	11
			L3	24 413.1	–	11

[a]From denatured native hemoglobin. Estimated errors ±1.5 for a1–a4 and ±3.0 for Dm.

[b]From reduced/Cam Hb. Estimated errors ±1.5 for a1–a4-Cys, b, c and d and ±3.0 for L1–L3. Masses are with Cys reduced.

[c]Comprises disulfide-bonded chains b and c. Reduced masses of chains b+c-6H (for four intra- and two inter-chain disulfide bonds)=31 971.8 Da. H, hydrogen.

[d]Unassigned, see text.

progressively higher affinities than W-Hb, whereas the reverse applies at higher pH.

Both hemoglobins express Bohr effects in the range pH 6.7–7.5. The Bohr factors in W-Hb vary inversely with temperature Φ=–0.48, –0.44 and –0.35 at 10, 20 and 30 °C, respectively, and exceed those in D (Φ=–0.11, –0.13 and –0.11, respectively).

W-Hb and D also differ in cooperativity coefficients, n_{50}. In W-Hb, the coefficient is higher, with a maximum at pH 7.5, and appears to vary inversely with temperature (n_{50}=2.5 at 10 °C, n_{50}=2.0 at 20 °C and n_{50}=1.8 at 30 °C). In D the value of n_{50} (1.2) is almost independent of pH.

Extended Hill plots of oxygen equilibria of the intact hemoglobin molecules (W-Hb) at pH 6.77 and 7.60 are shown in Fig. 9. The allosteric and other parameters derived from analysis of the equilibria in terms of the two-state Monod–Wyman–Changeux (MWC) allosteric model (as described by Weber et al., 1995) are given in Table 2. The correspondence between the cooperativity value at half-saturation (n_{50}) and the maximum cooperativity (n_{max}) and between P_{50} and the median oxygen affinity P_m (Table 2) reflects symmetrical oxygen-binding curves and permits the use of P_{50} values to analyse allosteric interactions. The control mechanism of the Bohr effect in this hemoglobin is primarily an increase in the oxygen-binding affinity of the hemoglobin in the oxygenated R ('relaxed') state (K_R) as pH rises, while the affinity (K_T) of the deoxygenated T ('tense') state remains relatively constant (Table 2). This raises the free energy of cooperativity (ΔG) (Table 2) and the K_T/K_R ratio with
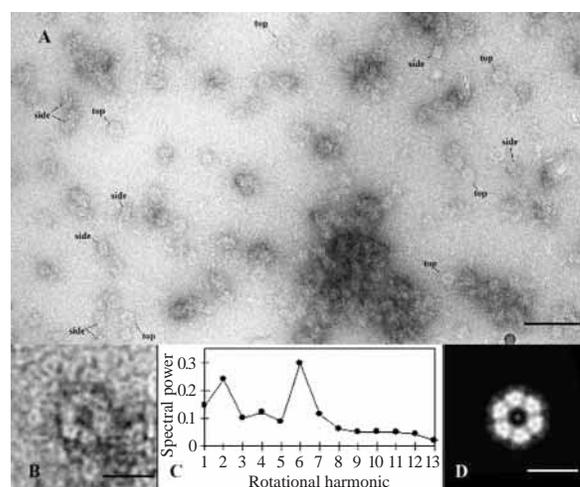

Fig. 6. Evidence for the hexagonal bilayer (HBL) structure of *Methanoaricia dendrobranchiata* hemoglobin. (A) Negatively stained electron microscope image of *M. dendrobranchiata* hemoglobin. The dark areas are stain. The protein of the molecular complex appears pale. The hemoglobin molecular complexes are in various orientations. The top and side views (indicated) appear to be similar to the top (sixfold) and side (twofold) views of other annelid hemoglobins. Scale bar, 200 nm. (B) An image of a typical top view taken from the electron microscope image in A. Scale bar, 30 nm. (C) Rotational frequency analysis of image B showing the strong sixfold symmetry expected of an HBL. (D) The sixfold rotationally Fourier-filtered image of B. The sub-structure, such as the density in the middle and the holes within the six subunits, is similar to that of other HBLs. Scale bar, 30 nm.
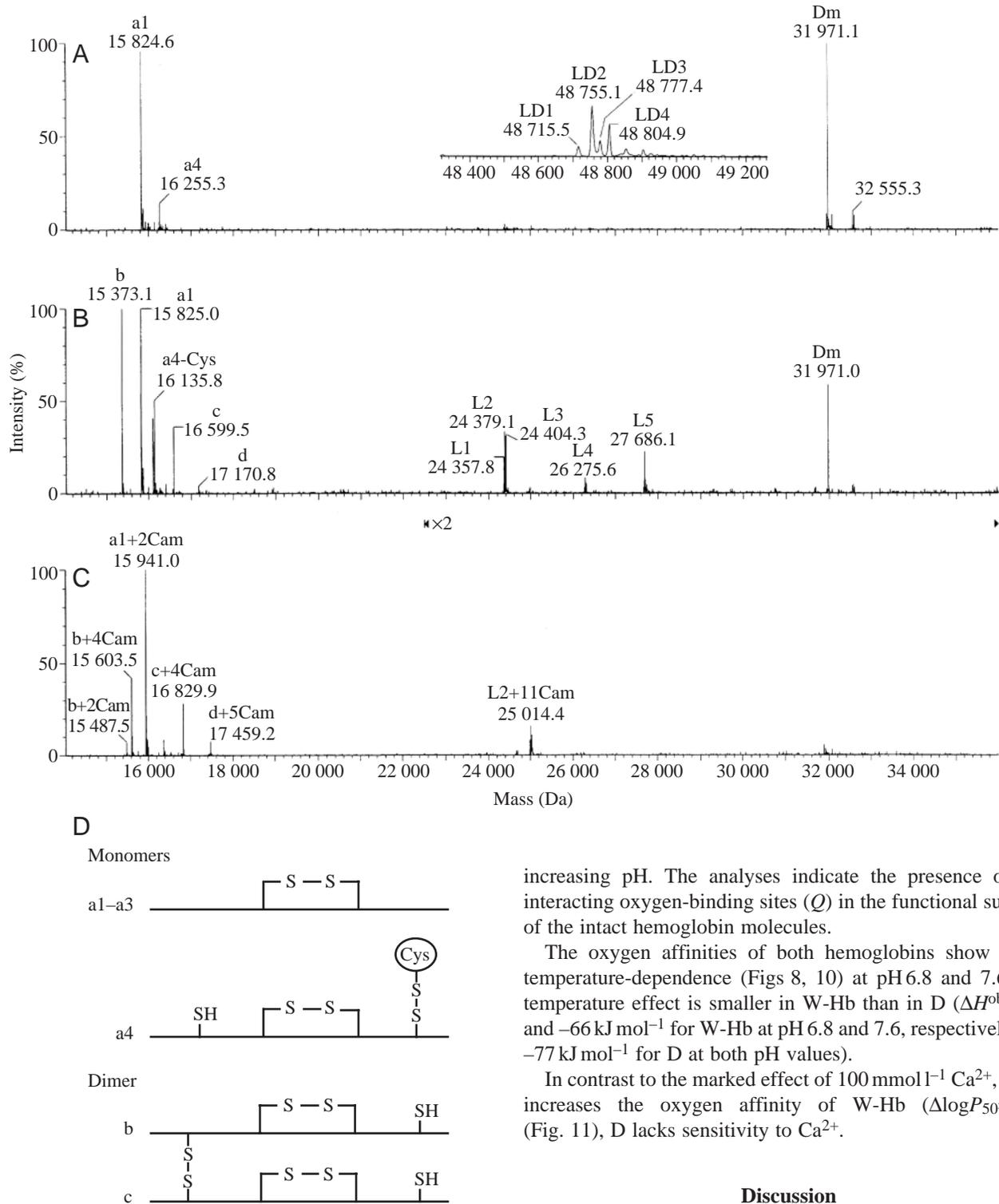
Fig. 7. Example mass spectra (one of five) of the 3.5×10⁶ Da hemoglobin under (A) non-reducing, (B) reducing and (C) reduced and carboxyamidomethylated (Cam) conditions. (D) Model of structure of the globin monomers and dimers. The inset in A shows the linker dimers on the same intensity scale as in A but on an expanded mass scale. a1–a4, b and c, globin chain subunits; LD1–LD4, linker dimers; Dm, globin dimer; ×2, portion of the spectrum where intensity has been multiplied by 2.

increasing pH. The analyses indicate the presence of 3–5 interacting oxygen-binding sites (Q) in the functional subunits of the intact hemoglobin molecules.

The oxygen affinities of both hemoglobins show strong temperature-dependence (Figs 8, 10) at pH 6.8 and 7.6. The temperature effect is smaller in W-Hb than in D ($\Delta H^{obs}=-58$ and $-66\,kJ\,mol^{-1}$ for W-Hb at pH 6.8 and 7.6, respectively, and $-77\,kJ\,mol^{-1}$ for D at both pH values).

In contrast to the marked effect of $100\,mmol\,l^{-1}\,Ca^{2+}$, which increases the oxygen affinity of W-Hb ($\Delta\log P_{50}=0.28$) (Fig. 11), D lacks sensitivity to Ca^{2+}.

Discussion

Methanoaricia dendrobranchiata is found in high densities at cold-seep sites often in association with mussels on the Upper Louisiana Slope (Blake, 2000; Smith et al., 2000). While this environment is characterized by a high local production (a strong trophic attractor), it provides harsh chemical conditions for the survival of metazoans (low oxygen and high sulfide concentrations). To survive and thrive under these conditions, the polychaetes must be adapted to take up

Table 2. *Monod–Wyman–Changeux and derived parameters for intact orbiniid hemoglobin molecules at pH 6.77 and 7.60*

pH	P_{50}	P_m	n_{50}	n_{max}	K_T	K_R	L	Q	ΔG
6.77	1.23	1.17	1.86	1.88	0.348 ± 0.0152	3.682 ± 0.573	570	4.34	5.29
7.60	0.58	0.59	1.86	1.86	0.366 ± 0.0713	6.958 ± 1.041	87	3.19	6.42

See Weber et al. (1995) for details of the curve-fitting and calculations.

K_T, oxygen association constant of the low-affinity state (T, tense); K_R, oxygen association constant of the high-affinity state (R, relaxed) (values are S.E. of the fitted parameters as estimated in the fitting procedure, the Levenberg–Morquordt method); L, allosteric constant; n_{50}, Hill's cooperativity coefficient; n_{max}, maximum cooperativity; P_{50}, oxygen pressure at half-saturation; P_m, median oxygen pressure; Q, number of interacting oxygen-binding sites; ΔG, free energy of heme–heme interaction.

oxygen at low environmental partial pressures and to tolerate anoxia and sulfide exposure.

Hemoglobin structure

Intact *Methanoaricia dendrobranchiata* hemoglobin has a native mass and appearance (as seen in transmission electron microscopy) typical of giant HBL annelid hemoglobins (for a review, see Lamy et al., 1996). On the basis of the masses of its dissociation products, it contains both globin and linker chains, as expected for HBL hemoglobins (for a review, see Lamy et al., 1996). There appear to be five linkers, although three of them (L1–L3) behave quite differently from the other two (L4 and L5) when reduced. Linkers L1–L3 possess 11

cysteine residues, 10 involved in intra-chain disulfide bonds and one involved in a disulfide bond between two linker chains (Table 1). All the linkers are dimeric, as in *Arenicola marina* (Zal et al., 1997), and are stable as monomers under reducing conditions. However, the other two linkers (L4 and L5), if indeed they are linkers, only appeared as monomers under mild reducing conditions and were never observed as either monomers or dimers in the native hemoglobin. Upon further reduction, they disappeared, and a number of components in the mass range 18–23 kDa were observed; these then disappeared after a longer reduction time. At this time, monomeric L1–L3 were still present, suggesting that L4 and L5 are significantly less stable than L1–L3. Both monomeric
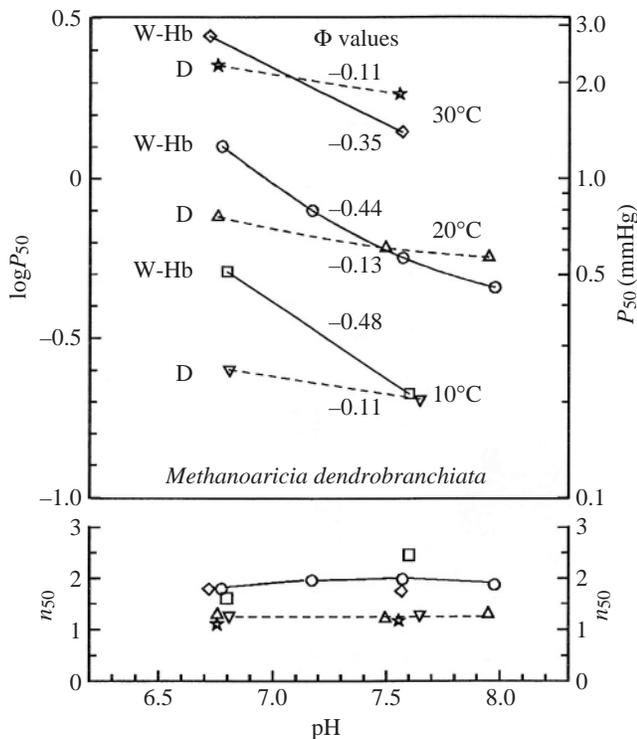

Fig. 8. Effect of pH on the affinity (P_{50} in mmHg; 1 mmHg=0.133 kPa) and cooperativity (n_{50}) of the intact hemoglobin (W-Hb) and putative dodecameric fraction (D) at 10, 20 and 30 °C. Numbers in italics show the Bohr factors (Φ) for the pH range 6.8–7.5. Buffer, 0.125 mol l⁻¹ Hepes in *Riftia* saline. Heme concentration, 0.51 mmol l⁻¹ (W-Hb) and 0.22 mmol l⁻¹ (D).
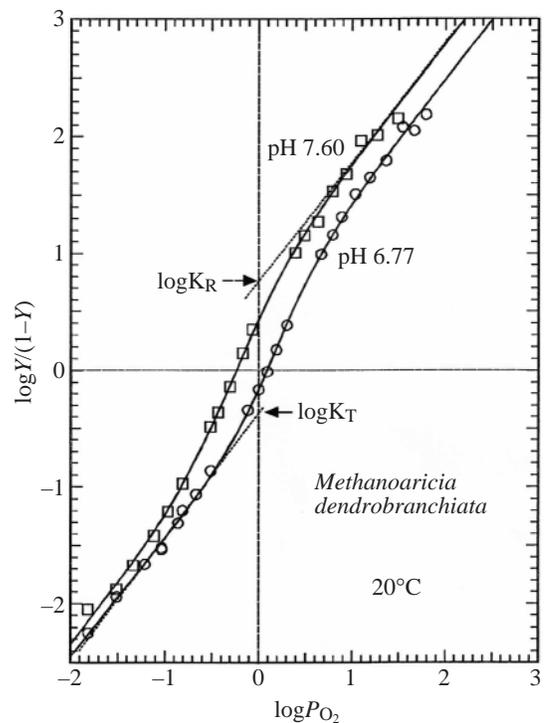

Fig. 9. Extended Hill plot of the intact hemoglobin at 20 °C pH 6.77 and 7.60. As indicated, the intersections between the lower and upper asymptotes to the Hill plot with the *y*-axis at $\log P_{O_2}=0$, indicate the values of $\log K_T$ and $\log K_R$, respectively. Other conditions as in Fig. 8. K_R, oxygen-binding affinity of the hemoglobin in the oxygenated (relaxed) state; K_T, oxygen-binding affinity of the hemoglobin in the deoxygenated (tense) state; *Y*, saturation.
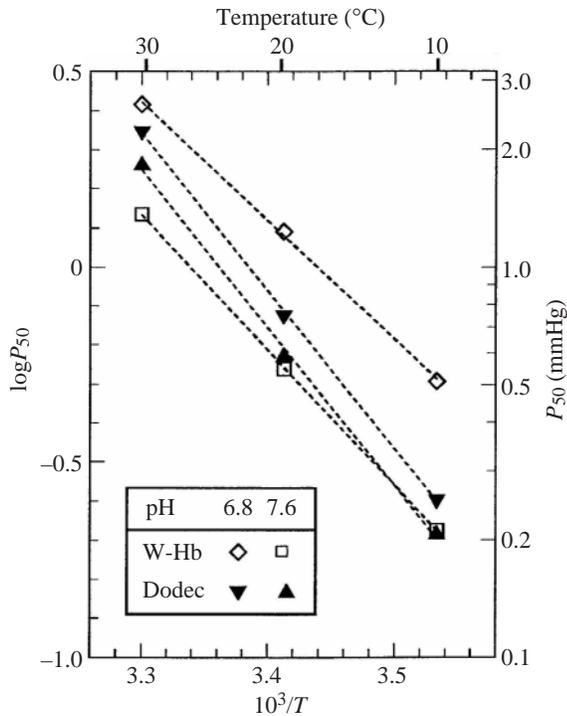
Fig. 10. Arrhenius plot for both the intact hemoglobin (W-Hb; open symbols) and the dodecameric fraction (Dodec; filled symbols) at pH 6.8 and 7.6. Other conditions as in Fig. 8. P_{50}, oxygen partial pressure at half-saturation; T, absolute temperature. 1 mmHg=0.133 kPa.

Fig. 11. Example of the effect of [Ca^{2+}] on the oxygen affinity (P_{50} in mmHg) and cooperativity (n_{50}) of the intact hemoglobin and its dodecamers at pH 7.0. Heme concentration, 0.32 mmol l^{-1}. W-Hb, intact hemoglobin; D, dodecameric fraction. 1 mmHg=0.133 kPa. Open columns, [Ca^{2+}]=0 mmol l^{-1}; stippled columns, [Ca^{2+}]=0.1 mmol l^{-1}.

(a1–a4) and dimeric (b and c) globins are present in *M. dendrobranchiata* hemoglobin. The globin dimers were unexpected because dimers have previously been considered to be typical of hirudinean (leech) and vestimentiferan hemoglobins in contrast to all other studied polychaetes, which possess globin trimers (for a review, see Lamy et al., 1996). This is also the first record of an annelid globin found to be cysteinylated. The origin of d remains unknown: it is probably involved in higher aggregation states, not detected by ESI-MS, or corresponds to a fragment of a linker, probably L4 or L5. A similar situation, where some subunits do not seem to ionize properly under non-reducing conditions, was encountered in *Eudistylia vancouverii* chlorocruorin (Green et al., 1998).

Functional properties

Both intact molecules and dodecamers exhibit similar and very high oxygen affinities but differ in other oxygen-binding characteristics (cooperativity, Bohr effect, sensitivity to Ca^{2+} and sensitivity to temperature). Their affinities are among the highest reported in annelids and probably represent adaptations to the animal's low-oxygen environment (Toulmond et al., 1990; Weber, 1978a, 1980; Toulmond, 1992; Hourdez et al., 1999, 2000; Weber and Vinogradov, 2001). The increase in K_R with rising pH (Fig. 9) is opposite to the situation for human hemoglobin (in which the Bohr effect is due to variation in K_T; Tyuma et al., 1973), but similar to that in the polychaete
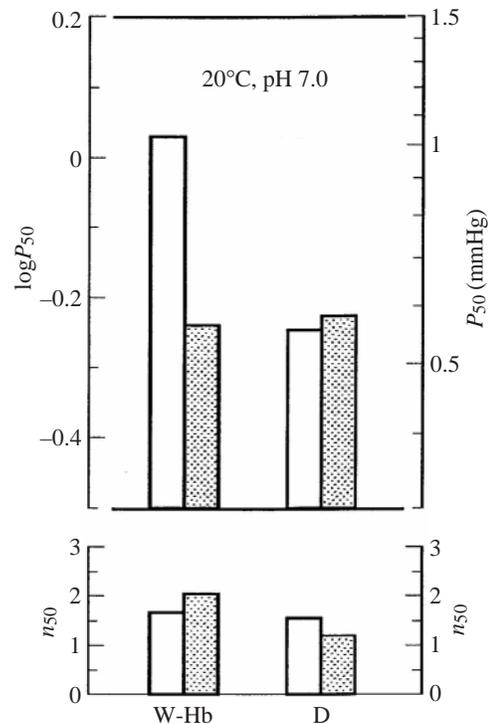
Arenicola marina, where it increases the Bohr factor at high oxygen saturation and favors oxygen saturation of blood entering the relatively alkaline gills (Weber, 1980; Toulmond, 1992).

The Bohr effect in the intact molecules (W-Hb) is similar to that of most extracellular hemoglobins (Weber, 1978a) but is greatly reduced in the dodecamer, as previously reported for other annelids (for a review, see Lamy et al., 1996).

In contrast to similar blood Ca^{2+} concentrations among vestimentiferans and other annelids studied (7–13 mmol l^{-1}), blood Mg^{2+} levels vary widely among species (from 2 to 44 mmol l^{-1}) (Oglesby, 1978; Sanders and Childress, 1991) and thus may affect the functional properties of annelid hemoglobins *in vivo*. Ca^{2+} increases the oxygen affinity of intact *M. dendrobranchiata* hemoglobin but has no effect on the dodecamers, suggesting that the effect of group IIA cations such as Ca^{2+} and Mg^{2+} involves the linkers. This agrees with other studies on HBL hemoglobin and most studies of dodecamers, with the exception of *Lumbricus terrestris* hemoglobin dodecamers, which are sensitive to group IIA cations (for a review, see Lamy et al., 1996). *Lumbricus terrestris* hemoglobin has been shown to have Ca^{2+}-binding sites with a variety of affinities that mainly involve linkers (Kuchumov et al., 2000). The low-affinity sites are likely to be involved in the effects of group IIA
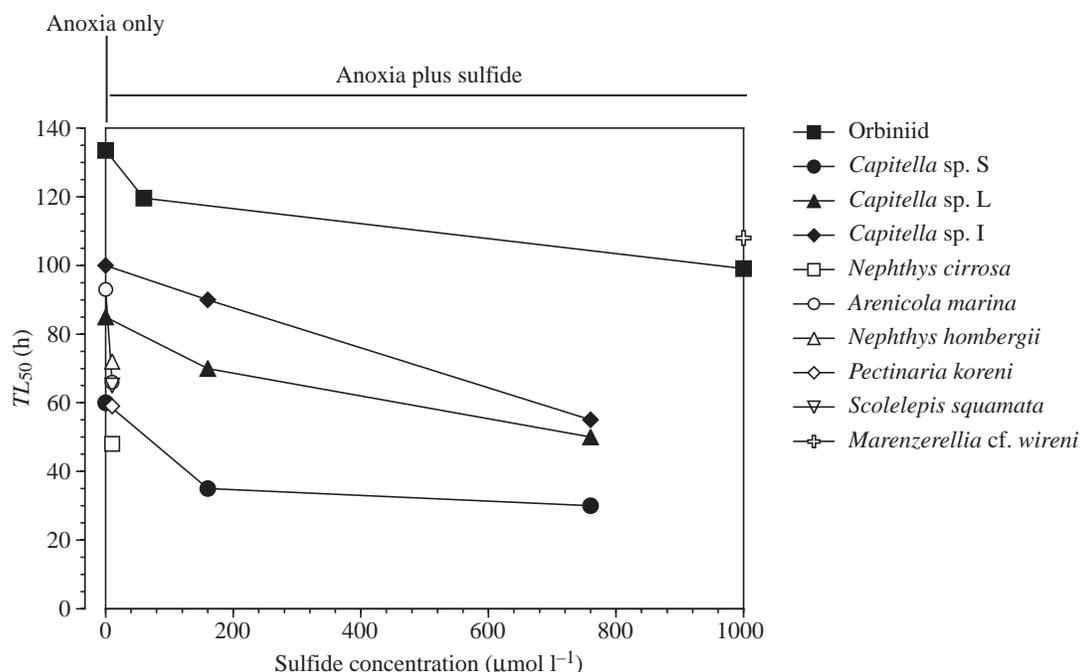
Fig. 12. Sulfide- and anoxia-tolerance in some polychaete species. Data from Schiedeck et al. (1997), Gamenick et al. (1998) and Groenendaal (1980) are also plotted. TL_{50}, 50 % survival rate. S. L and I are isolates in the *Capitella* species complex.

cations on the structure and function of hemoglobin (Kuchumov et al., 2000).

The cooperativity coefficients of *M. dendrobranchiata* hemoglobin are within the range previously reported for HBL hemoglobins (Weber and Vinogradov, 2001). The value for the intact molecule (2.5) is approximately twice that of the dodecamer (1.2), as seen in *Lumbricus terrestris* hemoglobin ($n{\approx}5$ and $n{\approx}2$, respectively, at pH 7.2; Krebs et al., 1996). The difference suggests a participation of the linker chains in heterotropic interactions in the molecule, as in other HBL hemoglobins (for a review, see Lamy et al., 1996).

The temperature-sensitivity of the intact hemoglobin ($\Delta H{=}{-}66\,\mathrm{kJ\,mol^{-1}}$ at pH 7.6) is similar to that of the polychaete *Abarenicola clarapedii*, another annelid that lives in a fairly stenothermal environment, but greater than that of *Arenicola marina* ($\Delta H{=}{-}22\,\mathrm{kJ\,mol^{-1}}$; Weber, 1972), which experiences larger temperature variations in its natural habitat. Given that dissociation of Bohr protons is endothermic and reduces the net heat liberated upon oxygenation of the hemes, the lower temperature effect in the whole molecules than in the dodecamers (Fig. 10) accords with the larger Bohr effect in the former. Analogously, ΔH^{obs} of the intact molecules is lower at pH 6.8 than at pH 7.6, where the Bohr effect is smaller (see Fig. 8).

Adaptations to the environment

The high affinity and strong Bohr effect observed in the vascular hemoglobin probably have adaptive significance in a low-oxygen environment, favoring both the binding of oxygen at the respiratory surfaces and its release in the tissues, where pH decreases as a result of the production of acid excretory products.

The oxygen consumption rates of *M. dendrobranchiata* are within the lower end of the normal range of respiratory rates reported for polychaetes (Childress and Mickel, 1985; Weber, 1978b). The worms are very good oxyregulators and are able to maintain a constant metabolic rate as environmental concentrations fall to $0.3\,\mathrm{mg\,O_2\,l^{-1}}$ (where $P_{\mathrm{O_2}}{=}870\,\mathrm{Pa}$) (Fig. 2). At lower partial pressures, the oxygen consumption rate drops sharply, and oxygen consumption ceases below $0.1\,\mathrm{mg\,O_2\,l^{-1}}$ ($P_{\mathrm{O_2}}{=}260\,\mathrm{Pa}$).

Strong oxyregulation extending to very low oxygen concentrations is normally correlated with one or more of the following adaptations: (i) a large gas-exchange surface, (ii) a short diffusion distance between the environment and the body fluids to facilitate gas diffusion, (iii) the presence of a respiratory pigment to increase the oxygen-carrying capacity of the circulating body fluid(s), (iv) a high oxygen affinity of the respiratory pigments to increase oxygen loading at low oxygen tension, (v) a high ventilatory rate to renew the medium as it becomes depleted of oxygen, and (vi) a high circulatory rate. *M. dendrobranchiata* have a large gill surface area and reduced diffusion distances across their respiratory surface as a result of intra-epidermal blood vessels in the gills (Hourdez et al., 2001). Furthermore, the worms are capable of greatly extending their gills when exposed to hypoxic and anoxic conditions (S. H., personal observation). The presence of cilia on the surface of the gills (Hourdez et al., 2001) facilitates renewal of the diffusion-limited water layer. These worms do not ventilate their gills, and no information is

available about ciliary movement under hypoxia. However, mussels from their natural habitat can create strong, small-scale currents.

M. dendrobranchiata hemoglobin has a very high oxygen affinity under physiological conditions; an oxygen partial pressure of 100 Pa, which is far below Pc, saturates the hemoglobin to 96 % at 10 °C *in vitro*. However, the oxygen consumption rate of *M. dendrobranchiata* decreases when the oxygen partial pressure falls below 870 Pa, probably as a result of diffusion-limitation driven by the decreased oxygen concentration gradient across their gills. However, this value (870 Pa) is low, indicating that the high oxygen affinity partially offsets the lack of ventilatory capability. The low P_c value reflects a high degree of oxyregulation, which is similar to that in *Riftia pachyptila* but slightly greater than those in the crab *Bythograea thermydron* and the clam *Calyptogena magnifica*, all from deep-sea hydrothermal-vent habitats (Childress and Fisher, 1992). Many deep-sea hydrothermal-vent and cold-seep microhabitats are characterized by low levels of dissolved oxygen, and endemic animals often show similar capacities to oxyregulate, delaying the onset of anaerobic metabolism.

Sulfide and anoxia-tolerance

Although the high mass-specific gill surface area favors oxygen uptake, it cannot selectively favor the entry of oxygen without permitting the inward diffusion of potentially harmful sulfide (Somero et al., 1989), which often occurs at substantial concentrations in the mussel beds (Smith et al., 2000; Nix et al., 1995). Sulfide further compromises respiration in most animals by inhibiting respiration at the level of cytochrome *c* oxidase and hinders binding of oxygen to most hemoglobins (Somero et al., 1989). The sulfide-tolerance under anoxia of these worms compares with that of *Marenzelleria* cf. *wireni* and is the highest found among the species studied to date (Fig. 12; Groenendaal, 1980; Schiedeck et al., 1997; Gamenick et al., 1998). The hemoglobin-bound oxygen store is not enough to sustain aerobic metabolism for more than 31 min. However, worms faced with prolonged anoxia switch to anaerobiosis and can survive for days even in the presence of sulfide.

Cold seeps, like hydrothermal vents, are habitats characterized by very high productivity and biomass compared with the generally nutrient-poor deep sea. The high level of endemism and low species-richness of these communities suggest that these environments are also physiologically challenging and that they require specific adaptations. We suggest that the ability of *Methanoaricia dendrobranchiata* to colonize their extreme environment is due at least in part to the adaptations reported here, such as their capacity to oxyregulate, which is due to the presence of a high-affinity hemoglobin, and their tolerance to anoxia and sulfide. These adaptations allow the worm to forage in the sulfidic, organic-rich sediments between and below the mussels and to exploit a habitat with little or no competition and limited predation (MacAvoy et al., 2002).

References

Arp, A. J., Doyle, M. L., Di Cera, E. and Gill, S. J. (1990). Oxygenation properties of the two co-occurring hemoglobins of the tube-worm *Riftia pachyptila*. *Respir. Physiol.* **80**, 323–334.

Blake, J. (2000). A new genus and species of polychaete worm (Family Orbiniidae) from methane seeps in the Gulf of Mexico, with a review of the systematics and phylogenetic interrelationships of the genera of Orbiniidae. *Cah. Biol. Mar*. **41**, 435–449.

Brooks, J. M., Kennicutt, M. C. I., Fisher, C. R., Macko, S. A., Cole, K., Childress, J. J., Bidigare, R. R. and Vetter, R. D. (1987). Deep-sea hydrocarbon seep communities: evidence for energy and nutritional carbon sources. *Science* **238**, 1138–1142.

Childress, J. J., Arp, A. J. and Fisher, C. R. (1984). Metabolic and blood characteristics of the hydrothermal vent tube-worm *Riftia pachyptila*. *Mar. Biol*. **83**, 109–124.

Childress, J. J. and Fisher, C. R. (1992). The biology of hydrothermal vent animals: physiology, biochemistry and autotrophic symbioses. *Oceanogr. Mar. Biol. Annu. Rev*. **30**, 337–441.

Childress, J. J., Fisher, C. R., Brooks, J. M., Kennicutt II, M. C., Bidigare, R. and Anderson, A. (1986). A methanotrophic marine molluscan symbiosis: mussels fueled by gas. *Science* **233**, 1306–1308.

Childress, J. J. and Mickel, T. J. (1985). Metabolic rates of animals from hydrothermal vents and other deep-sea habitats. *Biol. Soc. Wash. Bull.* **6**, 249–260.

Crowther, R. A., Henderson, R. and Smith, J. (1996). MRC image processing programs. *J. Struct. Biol.* **116**, 9–16.

Fisher, C. R. (1996). Ecophysiology of primary production at deep-sea vents and seeps. In *Biosystematics and Ecology Series*, vol 11, *Deep-Sea and Extreme Shallow-Water Habitats: Affinities and Adaptations* (ed. F. Uiblein, J. Ott and M. Stachowtisch), pp. 313–336. Vienna: Austrian Academy of Sciences Press..

Fisher, C. R., Childress, J. J., Arp, A. J., Brooks, J. M., Distel, D., Favuzzi, J. A., Felbeck, H., Fritz, L. W., Hessler, R., Johnson, K. S., Kennicutt II, M. C., Lutz, R. A., Macko, S. A., Newton, A., Powell, M. A., Somero, G. N. and Soto, T. (1988a). Variation in the hydrothermal vent clam, *Calyptogena magnifica*, at Rose Garden vent on the Galapagos rift. *Deep-Sea Res*. **35**, 1811–1832.

Fisher, C. R., Childress, J. J., Arp, A. J., Brooks, J. M., Distel, D., Favuzzi, J. A., Felbeck, H., Hessler, R., Johnson, K. S., Kennicutt II, M. C., Macko, S. A., Newton, A., Powell, M. A., Somero, G. N. and Soto, T. (1988b). Microhabitat variation in the hydrothermal vent mussel *Bathymodiolus thermophilus*, at Rose Garden vent on the Galapagos rift. *Deep-Sea Res*. **35**, 1769–1792.

Fisher, C. R., Fitt, W. K. and Trench, R. K. (1985). Photosynthesis and respiration in *Tridacna gigas* as a function of irradiance and size. *Biol. Bull*. **169**, 230–245.

Frank, J., Radermacher, M., Penczek, P., Zhu, P., Li, Y., Ladjadj, M. and Leith, A. (1996). SPIDER and WEB: processing and visualisation of images in 3D electron microscopy and related fields, *J. Struct. Biol*. **116**, 190–199.

Gamenick, I., Vismann, B., Grieshaber, M. K. and Giere, O. (1998). Ecophysiological differentiation of *Capitella capitata* (Polychaeta). Sibling species from different sulfidic habitats. *Mar. Ecol. Prog. Ser*. **175**, 155–166.

Green, B. N., Hutton, T. and Vinogradov, S. N. (1996). Analysis of complex protein and glycoprotein mixtures by electrospray ionization mass spectrometry with maximum entropy processing. In *Methods in Molecular Biology*, vol. 61, *Protein and Peptide Analysis by Mass Spectrometry* (ed. J. R. Chapman), pp. 279–294. Totowa, NJ: Humana Press Inc.

Green, B. N., Kuchumov, A. R., Klemm, D. J. and Vinogradov, S. N. (1999). An electrospray ionization mass spectrometric study of the giant, extracellular, hexagonal bilayer hemoglobin of the leech *Haemopsis grandis* provides a complete enumeration of its subunits. *Int. J. Mass. Spec.* **188**, 105–112.

Green, B. N., Kuchumov, A. R., Walz, D. A., Moens, L. and Vinogradov, S. N. (1998). A hierarchy of disulfide-bonded subunits: the quaternary structure of *Eudistylia* chlorocruorin. *Biochemistry* **37**, 6598–6605.

Grieshaber, M. K. and Völkel, S. (1998). Animal adaptations for tolerance and exploitation of poisonous sulfide. *Annu. Rev. Physiol.* **60**, 33–53.

Groenendaal, M. (1980). Tolerance of the lugworm (*Arenicola marina*) to sulphide. *Neth. J. Sea Res.* **14**, 200–207.

Hourdez, S., Frederick, L. A., Schernecke, A. and Fisher, C. R. (2001). Functional respiratory anatomy of a deep-sea orbiniid polychaete from the Brine Pool NR-1 in the Gulf of Mexico. *Invert. Biol.* **120**, 29–40.

Hourdez, S. and Jouin-Toulmond, C. (1998). Functional anatomy of the respiratory system of *Branchipolynoe* species (Polychaeta, Polynoidae), commensal with *Bathymodiolus* species (Bivalvia, Mytilidae) from deep-sea hydrothermal vents. *Zoomorphology* **118**, 225–233.

Hourdez, S., Lallier, F. H., De Cian, M.-C., Green, B. N., Weber, R. E. and Toulmond, A. (2000). The gas transfer system in *Alvinella pompejana* (Annelida Polychaeta, Terebellida). Functional properties of intracellular and extracellular hemoglobins. *Physiol. Biochem. Zool.* **73**, 365–373.

Hourdez, S., Lallier, F. H., Martin-Jézéquel, V., Weber, R. E. and Toulmond, A. (1999). Characterization and functional properties of the extracellular coelomic hemoglobins from the deep-sea hydrothermal vent scaleworm *Branchipolynoe symmytilida*. *Proteins* **34**, 435–442.

Johnson, K. S., Childress, J. J., Hessler, R. R., Sakamoto-Arnold, C. M. and Beehler, C. L. (1988). Chemical and biological interactions in the Rose Garden hydrothermal vent field. *Deep-Sea Res.* **35**, 1723–1744.

Jouin, C. and Gaill, F. (1990). Gills of hydrothermal vent annelids: structure, ultrastructure and functional implications in two alvinellid species. *Prog. Oceanogr.* **24**, 59–69.

Jouin-Toulmond, C., Augustin, D., Desbruyères, D. and Toulmond, A. (1996). The gas transfer system in alvinellids (Annelida, Polychaeta, Terebellida). Anatomy and ultrastructure of the anterior circulatory system and characterization of a coelomic, intracellular, haemoglobin. *Cah. Biol. Mar.* **37**, 135–151.

Kenney, J. M., von Bonsdorff, C.-H., Nassal, M. and Fuller, S. D. (1995). Conformational flexibility and evolutionary conservation in the Hepatitis B virus core structure. *Structure* **3**, 1011–1019.

Kennicutt II, M. C., Brooks, J. M., Bidigare, R. R., Fay, R. R., Wade, T. L. and McDonald, T. J. (1985). Vent-type taxa in a hydrocarbon seep region on the Louisiana Slope. *Nature* **317**, 351–353.

Krebs, A., Kuchumov, A. R., Sharma, P. K., Braswell, E. H., Zipper, P., Weber, R. E., Chottard, G. and Vinogradov, S. N. (1996). Molecular shape, dissociation and oxygen binding of the dodecamer subunit of *Lumbricus terrestris* hemoglobin. *J. Biol. Chem.* **271**, 18695–18704.

Kuchumov, A. R., Loo, J. A. and Vinogradov, S. N. (2000). Subunit distribution of calcium-binding sites in *Lumbricus terrestris* hemoglobin. *J. Prot. Chem.* **19**, 139–148.

Lamy, J. N., Green, B. N., Toulmond, A., Wall, J. S., Weber, R. E. and Vinogradov, S. N. (1996). The giant hexagonal bilayer hemoglobins. *Chem. Rev.* **96**, 3113–3124.

MacAvoy, S. E. R., Carney, R. S., Fisher, C. R and Macko, S. A. (2002). Use of chemosynthetic biomass by large, mobile, benthic predators in the Gulf of Mexico. *Mar. Ecol. Prog. Ser.* (in press).

MacDonald, I. R., Callender, R. W., Burke, R. A., Jr, McDonald, S. J. and Carney, R. S. (1990a). Fine-scale distribution of methanotrophic mussels at a Louisiana cold seep. *Prog. Oceanogr.* **24**, 15–24.

MacDonald, I. R., Guinasso, N. L., Reilly, J. F., Brooks, J. M., Callender, W. R. and Gabrielle, S. G. (1990b). Gulf of Mexico hydrocarbon seep communities. VI. Patterns in community structure and habitat. *Geo-Mar. Lett.* **10**, 244–252.

MacDonald, I. R., Reilly, J. F., Guinasso, N. L., Brooks, J. M., Carney, R. C., Bryant, W. A. and Bright, T. J. (1990c). Chemosynthetic mussels at a brine-filled pockmark in the northern Gulf of Mexico. *Science* **248**, 1096–1099.

Nix, E. R., Fisher, C. R., Vodenichar, J. and Scott, K. M. (1995).

Physiological ecology of a mussel with methanotrophic endosymbionts at three hydrocarbon seep sites in the Gulf of Mexico. *Mar. Biol.* **122**, 605–617.

Oglesby, L. C. (1978). Salt and water balance. In *Physiology of Annelids* (ed. P. J. Mill), pp. 555–658. London, New York, San Francisco: Academic Press.

Sanders, N. K. and Childress, J. J. (1991). The use of single column ion chromatography to measure ion concentrations in invertebrate body fluids. *Comp. Physiol. Biochem.* **98A**, 97–100.

Sarrazin, J. and Juniper, S. K. (1999). Biological characteristics of mosaic communities on hydrothermal edifices at Endeavour Segment, Juan de Fuca Ridge. *Mar. Ecol. Prog. Ser.* **185**, 1–19.

Schiedek, D., Vogan, C., Hardege, J. and Bentley, M. (1997). *Marenzelleria* cf. *wireni* (Polychaeta: Spionidae) from the Tay estuary. Metabolic response to severe hypoxia and hydrogen sulphide. *Aquat. Ecol.* **31**, 211–222.

Sick, H. and Gersonde, K. (1969). Method of continuous registration of O_2 binding curves of hemoproteins by means of a diffusion chamber. *Anal. Biochem.* **32**, 362–376.

Smith, E. B., Scott, K. M., Nix, E. R., Korte, C. and Fisher, C. R. (2000). Growth and condition of seep mussels (*Bathymodiolus childressi*) at a Gulf of Mexico Brine Pool. *Ecology* **81**, 2392–2403.

Somero, G. N., Anderson, A. E. and Childress, J. J. (1989). Transport, metabolism and detoxification of hydrogen sulfide in animals from sulfide-rich environments. *Rev. Aquat. Sci.* **1**, 591–614.

Toulmond, A. (1992). Properties and functions of extracellular heme pigments. In *Blood and Tissues Oxygen Carriers* (ed. C. P. Mangum), pp. 231–256. Berlin: Springer Verlag.

Toulmond, A., El Idrissi Slitine, F., De Frescheville, J. and Jouin, C. (1990). Extracellular hemoglobins of hydrothermal vent annelids: structural and functional characteristics in three alvinellid species. *Biol. Bull.* **179**, 366–373.

Tyuma, I., Kamigawara, Y. and Imai, K. (1973). pH dependence of the shape of the hemoglobin–oxygen equilibrium curve. *Biochim. Biophys. Acta* **310**, 317–320.

Valentine, R. G., Shapiro, B. M. and Stadtman, E. R. (1968). Regulation of glutamine synthetase. XII. Electron microscopy of the enzyme from *Escherichia coli*. *Biochemistry* **7**, 2143–2152.

Van Assendelft, O. W. (1970). Spectrophotometry of haemoglobin derivatives. Assen: Royal Vangorcum Ltd. 152pp.

Weber, R. E. (1972). On the variation in oxygen-binding properties of haemoglobins of lugworms (Arenicolidae, Polychaeta). In *Proceedings of the Fifth European Marine Biology Symposium* (ed. B. Battaglia), pp. 231–243. Padova, Italy: Editore Piccin.

Weber, R. E. (1978a). Respiratory pigments. In *Physiology of Annelids* (ed. P. J. Mill), pp. 393–446. London, New York, San Francisco: Academic Press.

Weber, R. E. (1978b). Respiration. In *Physiology of Annelids* (ed. P. J. Mill), pp. 369–392. London, New York, San Francisco: Academic Press.

Weber, R. E. (1980). Functions of invertebrate hemoglobins with special reference to adaptations to environmental hypoxia. *Am. Zool.* **20**, 79–101.

Weber, R. E. (1981). Cationic control of O_2 affinity in lugworm erythrocruorin. *Nature* **292**, 386–387.

Weber, R. E., Malte, H., Braswell, E. H., Oliver, R. W. A., Green, B. N., Sharma, P. K., Kuchumov, A. and Vinogradov, S. N. (1995). Mass spectrometric composition, molecular mass and oxygen binding of *Macrobdella decora* hemoglobin and its tetramer and monomer subunits. *J. Mol. Biol.* **251**, 703–720.

Weber, R. E. and Vinogradov, S. N. (2001). Nonvertebrate hemoglobins: Functions and molecular adaptations. *Physiol. Rev.* **81**, 569–628.

Wyman, J., Gill, S. J., Noll, L., Giardina, B., Colosimo, A. and Brunori, M. (1977). The balance sheet of a hemoglobin. Thermodynamics of CO binding by hemoglobin Trout I. *J. Mol. Biol.* **109**, 195–205.

Zal, F., Green, B. N., Lallier, F. H., Vinogradov, S. N. and Toulmond, A. (1997). Quaternary structure of the extracellular haemoglobin of the lugworm *Arenicola marina*. A multi-angle-laser-light-scattering and electrospray-ionisation-mass spectrometry analysis. *Eur. J. Biochem.* **243**, 85–92.

Zal, F., Lallier, F. H., Wall, J. S., Vinogradov, S. N. and Toulmond, A. (1996). The multi-hemoglobin system of the hydrothermal vent tube worm *Riftia pachyptila*. I. Re-examination of the number and masses of its constituents. *J. Biol. Chem.* **271**, 8869–8874.